Atmos. Meas. Tech. Discuss., 6, 5173–5194, 2013
www.atmos-meas-tech-discuss.net/6/5173/2013/
doi:10.5194/amtd-6-5173-2013
© Author(s) 2013. CC Attribution 3.0 License.

Atmospheric Measurement Techniques Discussions

This discussion paper is/has been under review for the journal Atmospheric Measurement Techniques (AMT). Please refer to the corresponding final paper in AMT if available.

Technical Note: Aeolian dust proxies produce visible luminescence upon intense laser-illumination that results from incandescence of internally mixed carbon

L. Ma, T. Cao, and J. E. Thompson

Department of Chemistry and Biochemistry, Texas Tech University, Lubbock, Texas, USA

Received: 19 April 2013 – Accepted: 29 May 2013 – Published: 12 June 2013

Correspondence to: J. E. Thompson (jon.thompson@ttu.edu)

Published by Copernicus Publications on behalf of the European Geosciences Union.

Abstract

Mineral dust mimics dispersed in air produced visible luminescence between 550–800 nm when illuminated with a high peak power (MW range) Nd:YAG laser beam at 532 or 1064 nm. The luminescence persists for a few microseconds after the laser pulse and the measured emission spectrum is roughly consistent with a blackbody emitter at ≈ 4300 K. Both observations are consistent with assigning laser-induced incandescence (LII) as the source of the luminescence. However, light emission intensity from the mineral dust proxies is 240–4600 less intense than incandescence from fresh kerosene soot on a per-mass basis at laser pulse energies < 25 mJ using a 1064 nm beam. The weak intensity of emission coupled with high emission temperature suggests a trace component of the sample may be responsible for the incandescence. To investigate further, we heated the soil samples in air to a temperature of 600 °C, and this treatment reduced light emission by > 90 % on average. Heating to 350 °C reduced emission by 45–72 %. Since black carbon soot and char (BC) oxidizes at elevated temperatures and BC is known to be present in soils, we conclude emission of light from the mineral dust aerosol proxies is likely a result of black carbon or char internally mixed within the soil dust sample. The reduction in LII response for samples heated to temperatures of 250–350 °C may result from partial oxidation of BC, but alternatively, could implicate a role for carbon present within organic molecules. The study suggests laser-induced incandescence measurements may allow quantitation of black carbon in soils and that soil dust is not truly an interferent in BC analysis by LII, but rather, a BC containing material.

1 Introduction

Laser-induced incandescence (LII) has recently become a popular method to measure atmospheric and laboratory generated black carbon (BC, soot) (Laborde et al., 2012a,b; Moteki and Kondo, 2007, 2010; Schwartz et al., 2010; Stephens et al., 2003).

AMTD
6, 5173–5194, 2013

The LII technique employs a high-peak-power pulsed laser to heat the light absorbing soot to temperatures of 2500–5000 °C within the 5–10 ns laser pulse. The soot reaches such high temperatures that it incandesces and produces broadband visible emission for up to 5 µs after the laser pulse. This relatively violent process irreversibly alters the physical structure of the soot containing particles (Michelson et al., 2007), however, the intensity of incandescence can be related to BC volume fraction or mass concentration through calibration. Often, impressive limits of detection for soot well below 1 ng m^{-3} of air can be achieved, and even single femtogram particles detected. This makes LII a very valuable measurement tool.

During recent experiments, we have noted mineral dust aerosol proxies also produce a measureable incandescence signal when illuminated by Nd:YAG laser light (both 532 and 1064 nm). This could indicate mineral dust might pose a possible interferent for BC analysis by LII, and this led us to investigate the phenomenon further. This report is the product of this investigation. The manuscript that follows serves the community by documenting the initial observation of LII from dust proxies, by providing relative LII signal responses for typical mineral dust samples as compared to soot at equivalent light absorption/mass concentration, and by unravelling the mechanism by which the LII signal is produced. The resultant data and analysis suggests BC present within soil as char or soot is the likely cause of the majority of the incandescence signal intensity observed. This conclusion suggests LII may be a useful technique to quantify BC in soils, and enhanced LII signals observed during intense dust episodes may largely result from suspension of BC containing material during the process of wind erosion.

2 Methods

2.1 Mineral dust proxies, sample handling, and aerosol generation

Pullman and Amarillo soil samples were collected exactly as described in Ma et al. (2011). These soil types are native to the Texas panhandle. Additional samples

AMTD
6, 5173–5194, 2013

tested included a soil collected from the upper 5 cm of soil from a farm in Michigan (here termed "MSA") and Whole Grain Silica OK #1 sand (T&S Material, Gainesville, TX). Prior to analysis the soils were passed through a 250 micron sieve to remove the largest particles. Soils were tested (1) as sieved, and (2) after heating at either 110, 250, 350 or 600 °C for 14 h in a temperature controlled oven. Heating occurred in air where both volatilization of material and chemical oxidation could occur.

The mineral dust aerosol samples were then dispersed in HEPA filtered air by mechanically stirring a small quantity of the dust placed into a sealed Pyrex flask. The dust was drawn into the LII optical chamber through 3/8" conductive tubing and through an internal glass tube that comprises the sample optical cell for LII analysis. The aerosol was then drawn through an additional short length (approx. 0.5 m) of conductive tubing and split using a tee. A portion of the sample was directed to the particle soot absorption photometer (PSAP) and the remaining sample was directed into a mass concentration monitor (RAM-1, Mie Inc.) that reported the aerosol mass in $mg\,m^{-3}$. Sample flow rates were approx. 1.5 L per minute (LPM) into the PSAP and 2 LPM into the concentration monitor. Soot aerosol was generated within a fume hood by burning Coleman brand kerosene in a lantern commonly used for camping. The soot produced was sampled through an approx. 20 m length of tubing that allowed cooling and into the optical measurement apparatus after variable dilution into filtered room air as needed.

2.2 Optical and aerosol particle measurements

The optical chamber for LII was a flow-through integrating sphere depicted in Fig. 1 and described previously in detail (Dial et al., 2010; Qian et al., 2012; Ma and Thompson, 2012; Thompson et al., 2008; Redmond and Thompson, 2011). Laser light was directed along the axis of the glass tube through the sphere. One modification to the experiment compared to the previous literature was no interference filter was used prior to the photomultiplier tube (PMT). A second modification is that VIS and near-IR transparent windows were used to form the ends of the optical cell. A visible light-blocking filter (FGL850, Thor Labs) was used to remove both 532 nm laser light and any residual

AMTD
6, 5173–5194, 2013

flash lamp emission from the Nd:YAG laser beam (BRIO Laser, Big Sky/Quantel) for many experiments. As a result, only 1064 nm light was used to induce incandescence for all experiments unless otherwise specifically noted. The photomultiplier tube current was converted to a voltage through a 500Ω load and measured using a 100 MHz, 8-bit oscilloscope (Tektronix 1012B) triggered by the laser's Q-switch. The peak-to-peak incandescence signal was logged by the scope, and we have used this variable to quantitate incandescence intensity for all samples. A 3λ Particle/Soot Absorption Photometer (PSAP, Radiance Research, Seattle, WA) was placed at the outlet of the LII optical cell to monitor light absorption by aerosols on the green channel at 530 nm. The green channel was used since mass absorption cross sections ($m^2\,g^{-1}$) for soot and dust aerosols have previously been reported as 13.1 and 0.05 $m^2\,g^{-1}$ for this spectral region in the literature (Subramanian et al., 2010; Linke et al., 2006). These values allow conversion between light absorption coefficient observed by the PSAP (Mm^{-1}) and aerosol mass concentration ($\mu g\,m^{-3}$). This conversion was done exclusively for soot aerosol that was present at too low a concentration to reliably measure with the mass concentration monitor we used. We have also developed our own values for soil dust absorption cross sections based on data collected (see Table 1). For some experiments, a scanning mobility particle sizing system (SMPS, TSI 3080) and/or condensation particle counter (CPC, TSI 3772) was placed at the LII cell outlet. This was used to monitor changes in size distribution or particle concentration induced by lasing. Sample flow into the SMPS was always < 1 LPM, and at minimum a 1 : 10 ratio between sample flow and sheath flow was maintained. To collect the emission spectra of dusts, a few grams of soil dust was piled onto a support and directly illuminated with either the 532 nm laser beam or the 1064 nm beam. A 0.25″ diameter lens was placed within a few cm of the illuminated spot and used to collect light emission from the dust sample under direct irradiation by the laser beam. Dust emission spectra were acquired via an Ocean Optics Jaz Spectrometer through a 1 m length of optical fiber (1 mm core diameter).

AMTD
6, 5173–5194, 2013

3 Results and discussion

3.1 Qualitative characteristics of emission from mineral dust proxies

Figure 2 illustrates emission spectra of bulk Pullman and Amarillo soils after illumination with light from a Nd:YAG laser (both 532 or 1064 nm irradiation shown here). For this experiment, a few grams of dust was placed on a support and illuminated directly with the laser beam. Scatter from the laser line at 532 nm is evident in the figure as an off-scale peak in the green traces. Visible emission is noted between approx. 580–800 nm for both dust samples at both wavelengths. The emission from the dust when illuminated at 1064 nm was easily visible with the unaided eye through laser goggles, and a photograph of the emission could easily be recorded with a cellular phone camera as illustrated in the figure. For comparison, we also include the expected emission profile from a blackbody at 4300 K in the data plot of Fig. 2 as expected from the Wein's displacement law. This data is plotted in black, and on a second y-axis (not shown) for scaling. The broadband nature of emission from the dust suggests incandescence may be responsible for the light emission. These experiments on the bulk, non-dispersed dust also suggest vaporization of some material occurs (clearly visible to observer) and repeat illumination of the sample at the same location rapidly decreased the brightness of luminescence (within 5–10 s). However, luminescence never ceased completely. Figure 3 illustrates the time response for light emission for a dispersed dust sample contained within the integrating sphere. As observed, visible emission persisted for a few microseconds after the laser pulse. This result is also consistent with laser-induced incandescence being the cause of light emission. Figure 3 also defines the peak-to-peak signal we have employed for quantitative measurements of emission used later in our discussion (Sect. 3.2 and elsewhere).

AMTD
6, 5173–5194, 2013

3.2 Quantitative characteristics of emission from mineral dust proxies

To describe the emission intensity observed we have performed experiments in which the different soil dust samples were analysed by LII and also measured via a PSAP and mass concentration monitor. To account for variations in mass concentrations between samples we have constructed plots of observed LII peak-peak signal vs. mass concentration and vs. PSAP absorbance. The resulting slope of a best-fit line between the variables was then determined. This procedure normalized the LII signal intensities observed by dividing by either the mass concentration measured and/or the PSAP absorption signal for the green channel. Figure 4 reports an example of the type of plots constructed. In this figure, the LII emission intensities for the Amarillo and Pullman soil sample dusts and for fresh kerosene soot are plotted as a function of aerosol mass concentration. Here we use identical y-axis scaling for direct comparison of LII signal intensity. Mass concentrations were not measured directly in this particular experiment, but rather, we convert to mass concentration by using PSAP data and mass absorption cross sections of 0.27, 0.25, and 13.1 $m^2\,g^{-1}$ for Amarillo soil dust, Pullman soil dust and soot, respectively. The values used for the soil dusts were determined in our experiments by relating the PSAP and mass concentration data. A second x-axis also provides PSAP absorption data for reference. Additional experimental results of this type are summarized in Table 1. As observed in the table and figure, fresh soot produces incandescence that is always several orders of magnitude brighter than the soil dusts we tested on a per-mass basis. As previously mentioned, the observed peak in the emission spectrum from the dust samples was consistent with an emitter at approx. 4300 °C – a temperature very similar to what soot achieves during LII. However, the emitted power from a blackbody also scales with temperature – so we should expect similar incandescence intensity for both soot and the mineral dusts if the soil dust sample behaves as a homogenous sample at equivalent temperature. However, the data of Fig. 4 and Table 1 indicate this was not observed and soil dust emission was always much lower than fresh kerosene soot. An explanation for the data set is that

AMTD
6, 5173–5194, 2013

a minor component in the mineral dust sample is responsible for the majority of the incandescence observed. This hypothesis is explored further in Sect. 3.3.

3.3 The source of incandescence emission from soil dust proxies

One potential source of the observed incandescence is the possibility that BC (also soot, char – here we use these terms as synonyms) is present in the dust samples we have used. Contamination could occur by the mineral dust coming into contact with soot that was present in tubing connections or in the optical cell itself prior to measurement. However, we have been able to eliminate this as a possibility since sodium chloride dust added to the measurement system in the same way as the mineral dust produced no incandescence signal and we feel any physical/abrasive type of contamination process would be equivalent for the two samples. A second possibility is that soot may be natively present in the soil itself. Soil and sediments are known to contain char and soot deposited as a result of anthropogenic emissions or biomass burning (Schmidt and Noack, 2000; Chia et al., 2012; Han et al., 2012). Therefore, we may fully expect an incandescence signal from the BC present within the soil sample itself.

To test this possibility we have heated the mineral dust samples within a crucible. Heating took place in a temperature-controlled oven, or on some occasions within a Bunsen burner flame to allow even more vigorous heat treatment. BC is known to degrade during prolonged exposure to temperatures $> 550^{\circ}$C in air (Gustafsson et al., 1996; Lu et al., 2012). This thermal treatment allows a means to effectively remove soot and organic material from the mineral dust sample prior to testing for LII response. Obvious physical changes accompanied heating to 600 $^{\circ}$C as all dust samples except the sand visually changed appearance (see Fig. 5b). The heated soil dusts were then introduced into the optical cell and the LII signal response per unit mass or absorption was found to be reduced by > 90 % on average for samples heated to 600 $^{\circ}$C (see Table 1 for data). This suggests that the material responsible for incandescence was largely lost or otherwise made inactive during heating to 600 $^{\circ}$C. However, no amount of heating (even at much higher temperatures in burner flame) was found to completely elimi-

AMTD
6, 5173–5194, 2013

nate incandescence. Slopes of the LII response lines as a function of indicated mass concentration could be reduced to the 10^{-2} mV m^3 mg^{-2} range with vigorous heating. Thus, the response of soot on a per mass basis is often $> 10^4$ fold greater than that of vigorously heated mineral dusts. This result could suggest the refractory light absorbing mineral dust maintains some ability to incandesce very weakly. Another possibility is that a small amount of recalcitrant BC escapes oxidation and remains in the sample. The LII response loss at additional temperatures was also determined and this data is presented in Fig. 5. Heating the samples to only 350 °C reduced LII emission per unit mass by 45–72 %. Heating to 250°C reduced LII emission by 21 % on average, while heating to 110 °C was actually found to enhance LII emission by approximately 7 % on average. However, this enhancement was not thought to be statistically relevant due to a large range of values observed. The conclusion reached is that a component within the sample that volatilizes or oxidizes below 600 °C is largely responsible for the observed incandescence of the soils tested. Inspection of the photographs in Fig. 5b indicate large changes in soil color also occur, and this change is most dramatic between 350–600 °C. Black carbon or char present in the sample is known to oxidize in a similar temperature range, and it appears as if this component of the soil may be responsible for the LII signal observed. However, we also observed substantial loss of LII signal at temperatures of 250–350 °C. This temperature is lower than that at which atmospheric soot is believed to oxidize. However, differential scanning calorimetry (DSC) data for a variety of soils and chars has illustrated exothermic reactions begin to occur at temperatures as low as 200 – 250^o C during heating in air (Barros et al., 2007; Critter and Airoldi, 2006; Barros et al., 2011; Tia et al., 1991). These reactions have been attributed to the oxidation/combustion of organic material within the samples. It is certainly possible that the light absorbing BC in soils exhibits substantially different chemical properties compared to atmospheric soot, and perhaps begins to oxidize at a lower temperature. A second possibility is that a portion of the LII response can be attributed to organic molecules in the sample that are removed by the 250–350 °C heat-

AMTD
6, 5173–5194, 2013

ing step. The exact mechanism by which the organic molecules could enhance LII is unknown, but if present we speculate it could be pyrolytic in nature.

3.4 The physical alteration of dust proxies during laser irradiation

Figure 6 illustrates a series of physical changes observed when dust samples are irradiated with the combined 532 + 1064 nm beam. The images depict an experiment in which Pullman dust was deposited onto a glass microscope slide and imaged using a light microscope before and after lasing. The region shown in both images is the same. A faint "L" shaped feature can be seen near the center of both images. Significant changes can be observed between the two images. Some dust particles/granules can be observed to change shape or size (many get smaller) as a result of illumination. Several of these particles are highlighted with small arrows in the figure. In addition, new particles seem to appear in the field of view after illumination, and the density of particles on the slide seems to increase by roughly 50 %. Taken together, the micrographs suggest the dust undergoes a complex and significant restructuring during illumination that may include particle volatilization and fragmentation. These results are also consistent with the additional data presented in Fig. 6 for dispersed dust lased with 532 + 1064 nm. The particle size distribution of Pullman dust measured with a scanning mobility particle sizing system was observed to shift to smaller diameters as a result of lasing. In addition, the bar graphs of Fig. 6 illustrate particle count/concentration increases significantly when Pullman dust was lased. For this experiment, a CPC was placed at the outlet of the LII optical cell and count data was recorded for non-lased dust. Then, the laser was turned on and immediately a large increase in particle concentration was noted. The results illustrated in Fig. 6 are quite similar to results reported by Michelson et al. (2007) when performing LII measurements on soot. Those authors reported a large number of very small new particles form when soot is lased by a Nd:YAG beam. The results of Fig. 6 all support the conclusion that lasing the dust sample with the Nd:YAG beam caused a significant alteration in the aerosol sample.

AMTD
6, 5173–5194, 2013

In addition, the formation of new particles is similar to what was observed when soot aerosol was tested as in Michelson et al. (2007).

4 Conclusions

The data suggests the material responsible for causing laser-induced incandescence of soil dust proxies is largely removed from a soil sample when heated in air at temperatures between 250° and 600 °C. Particle size distribution measurements suggest a significant number of new particles form during lasing, and a similar effect has previously been observed for soot in LII measurements. All experimental results are consistent with a carbonaceous component present in the soil dust at low mass concentration causing the majority of the observed LII. After vigorous heating, the soil dusts tested exhibited LII responses more than 10^4 times lower than kerosene soot on a per-mass basis. After vigorous heating, the soil dusts tested exhibited LII responses more than 10^4 times lower than kerosene soot on a per-mass basis for the visible light detected by the photomultiplier tube. As such, it appears the refractory portion of mineral dust aerosol cannot reasonably be considered an interferent in atmospheric BC analysis by ensemble LII measurements – even during extreme dust events. However, it is certainly possible that BC materials present within soils may become dispersed during periods of wind erosion, and this material might produce a measureable signal via LII. Therefore, soil dust aerosol should be considered a material that potentially contains BC, and the wind erosion mechanism of BC dispersion warrants additional investigation.

Acknowledgements. The authors thank Ed Quitevis and Lianjie Xue for offering use of the temperature controlled furnace for this work. In addition, Ted Zobeck of the USDA-ARS lab generously provided the soil samples and sieve used in this study. The authors acknowledge the State of Texas/Texas Tech University (TTU) and the National Science Foundation (NSF, award 1004114) for financial support of our research. However, the views expressed in this manuscript do not necessarily represent those of TTU or NSF. All authors contributed to col-

AMTD
6, 5173–5194, 2013

lecting and analysing experimental data. J. E. Thompson authored the manuscript with editing by L. Ma and T. Cao.

References

Barros, N., Salgado, J., and Feijoo, S.: Calorimetry of Soil, Thermochim. Acta, 458, 11–17, 2007.

Barros, N., Salgado, J., Villanueva, M., Rodriquez-Anon, J., Proupin, J., Feijoo, S., and Martin-Pastor, M. J.: Application of DSC-TG and NMR to study the soil organic matter, J. Therm. Anal. Calorim., 104, 53–60, 2011.

Chia, C. H., Munroe, P., Joseph, S. D., Lin, Y., Lehmann, J., Muller, D. A., Xin, H. L., and Neves, E.: Analytical electron microscopy of black carbon and microaggregated mineral matter in Amazonian dark Earth, J. Microscopy, 245, 129–139, 2012.

Critter, S. A. M. and Airoldi, C.: Thermal Analysis of Brazilian Tropical Soils Originating from Different Sources, J. Braz. Chem. Soc., 17, 1250–1258, 2006.

Dial, K., Hiemstra, S., and Thompson, J. E.: Simultaneous Measurement of Optical Scattering and Extinction on Dispersed Aerosol Samples, Anal. Chem., 82, 7885–7896, 2010.

Gustafsson, O., Haghseta, F., Chan, C., MacFarlane, J., and Gschwend, P. M.: Quantification of the Dilute Sedimentary Soot Phase: Implications for PAH Speciation and Bioavailability, Environ. Sci. Technol., 31, 203–209, 1996.

Han, Y. M., Marlon, J. R., Cao, J. J., Jin, Z. D., and An, Z. S.: Holocene linkages between char, soot, biomass burning and climate from Lake Daihai, China, Global Biogeochem. Cy., 26, GB4017, doi:10.1029/2011GB004197, 2012.

Laborde, M., Mertes, P., Zieger, P., Dommen, J., Baltensperger, U., and Gysel, M.: Sensitivity of the Single Particle Soot Photometer to different black carbon types, Atmos. Meas. Tech., 5, 1031–1043, doi:10.5194/amt-5-1031-2012, 2012a.

Laborde, M., Schnaiter, M., Linke, C., Saathoff, H., Naumann, K.-H., Möhler, O., Berlenz, S., Wagner, U., Taylor, J. W., Liu, D., Flynn, M., Allan, J. D., Coe, H., Heimerl, K., Dahlkötter, F., Weinzierl, B., Wollny, A. G., Zanatta, M., Cozic, J., Laj, P., Hitzenberger, R., Schwarz, J. P., and Gysel, M.: Single Particle Soot Photometer intercomparison at the AIDA chamber, Atmos. Meas. Tech., 5, 3077–3097, doi:10.5194/amt-5-3077-2012, 2012b.

AMTD
6, 5173–5194, 2013

Linke, C., Möhler, O., Veres, A., Mohácsi, Á., Bozóki, Z., Szabó, G., and Schnaiter, M.: Optical properties and mineralogical composition of different Saharan mineral dust samples: a laboratory study, Atmos. Chem. Phys., 6, 3315–3323, doi:10.5194/acp-6-3315-2006, 2006.
Lu, T., Cheung, C. S., and Huang, Z.: Investigation on Particulate Oxidation from a DI Diesel Engine Fueled with Three Fuels, Aerosol Sci. Tech., 46, 1349–1358, 2012.
Ma, L. and Thompson, J. E.: Optical Properties of Dispersed Aerosols in the Near UV (355 nm): Measurement Approach and Initial Data, Anal. Chem., 84, 5611–5617, 2012.
Michelson, H. A., Tivanski, A. V., Gilles, M. K., van Poppel, L. H., Dansson, M. A., and Buseck, P. R.: Particle formation from pulsed laser irradiation of soot aggregates studied with a scanning mobility particle sizer, a transmission electron microscope, and a scanning transmission x-ray microscope, Appl. Optics, 46, 959–977, 2007.
Moteki, N. and Kondo, Y.: Effects of mixing state on black carbon measurements by laser-induced incandescence, Aerosol Sci. Tech., 41, 398–417, 2007.
Moteki, N. and Kondo, Y.: Dependence of laser-induced incandescence on physical properties of black carbon aerosols: measurements and theoretical interpretation, Aerosol Sci. Tech., 44, 663–675, 2010.
Qian, F., Ma, L., and Thompson, J. E.: Angular Truncation Corrections for the Aerosol Albedometer: Modeling & Laboratory Measurements of Scattering Correction Factors, J. Eur. Opt. Soc. – Rapid Publications, 7, 12021, 2012.
Redmond, H. and Thompson, J. E.: Evaluation of a Quantitative Structure Property Relationship (QSPR) for Predicting Mid-Visible Refractive Index of Secondary Organic Aerosol (SOA), Phys. Chem. Chem. Phys., 13, 6872–6882, 2011.
Schmidt, M. W. I. and Noack, A. G.: Black carbon in soils and sediments: Analysis, distribution, implications, and current challenges, Global Biogeochem. Cy., 14, 777–793, doi:10.1029/1999GB001208, 2000.
Schwartz, J. P., Spackman, J. R., Gao, R. S., Perring, A. E., Cross, E., Onasch, T. B., Ahern, A., Wrobel, W., Davidovits, P., Olfert, J., Dubey, M. K., Mazzoleni, C., and Fahey, D. W.: The detection efficiency of the single particle soot photometer, Aerosol Sci. Tech., 44, 612–628, 2010.
Stephens, M., Turner, N., and Sandberg, J.: Particle identification by laser-induced incandescence in a solid-state laser cavity, Appl. Optics, 42, 3726–3736, 2003.
Subramanian, R., Kok, G. L., Baumgardner, D., Clarke, A., Shinozuka, Y., Campos, T. L., Heizer, C. G., Stephens, B. B., de Foy, B., Voss, P. B., and Zaveri, R. A.: Black carbon over Mex-

AMTD
6, 5173–5194, 2013

ico: the effect of atmospheric transport on mixing state, mass absorption cross-section, and BC/CO ratios, Atmos. Chem. Phys., 10, 219–237, doi:10.5194/acp-10-219-2010, 2010.
Thompson, J. E., Barta, N., Policarpio, D., and DuVall, R.: Development of a Fixed Frequency Aerosol Albedometer, Opt. Express, 16, 2191–2205, 2008.
Tia, S., Bhattacharya, S. C., and Wibulswas, P.: Thermogravimetric Analysis of Thai Lignite – II. Char Combustion Kinetics, Energy Convers. Mgmt., 31, 277–284, 1991.

AMTD
6, 5173–5194, 2013

Table 1. Quantitative results.

Sample	LII Intensity ($mV\,m^3\,mg^{-1}$)	LII Intensity $\times 10^3$ ($mV\,Mm^{-1}$)	Mass absorption cross section ($m^2\,g^{-1}$)
MSA-not heated	3.3 ± 0.8	5 ± 1.1	0.75[a]
MSA – 14 h @ 350 C[b]	1.8 ± 0.2	2.4 ± 0.3	
MSA – 14 h @ 600 C[b]	0.029 ± 0.005	0.19 ± 0.05	
Sand-not heated	0.35 ± 0.06	3.0 ± 0.5	0.11[a]
Sand – 14 h @ 350 C[b]	0.17 ± 0.03	1.5 ± 0.3	
Sand – 14 h @ 600 C[b]	0.07 ± 0.05	0.73 ± 0.47	
Amarillo-not heated	0.26 ± 0.03	1.1 ± 0.16	0.27[a]
Amarillo – 14 h @ 350 C[b]	0.10 ± 0.01	0.36 ± 0.05	
Amarillo – 14 h @ 600 C[b]	0.017 ± 0.004	0.067 ± 0.018	
Pullman – not heated	0.17 ± 0.01	0.8 ± 0.06	0.25[a]
Pullman – 14 h @ 350 C[b]	0.048 ± 0.004	0.23 ± 0.04	
Pullman – 14 h @ 600 C[b]	0.011 ± 0.003	0.07 ± 0.02	
Fresh Kerosene Soot	800 ± 30	–	13.1[c]

± uncertainty is the 95 % confidence intervals of best-fit slopes.
[a] Mass absorption cross-section is from the green channel for the PSAP and mass concentration monitor data.
[b] Observed mass loss upon heating to 350 °C were: MSA: 50 % loss; sand: 0.01 % loss; Amarillo: 1.25 % loss; Pullman: 4.3 % loss. Samples were not dried prior to this analysis.
[c] M. A. C. value is from Subramanian et al. (2010).

AMTD
6, 5173–5194, 2013

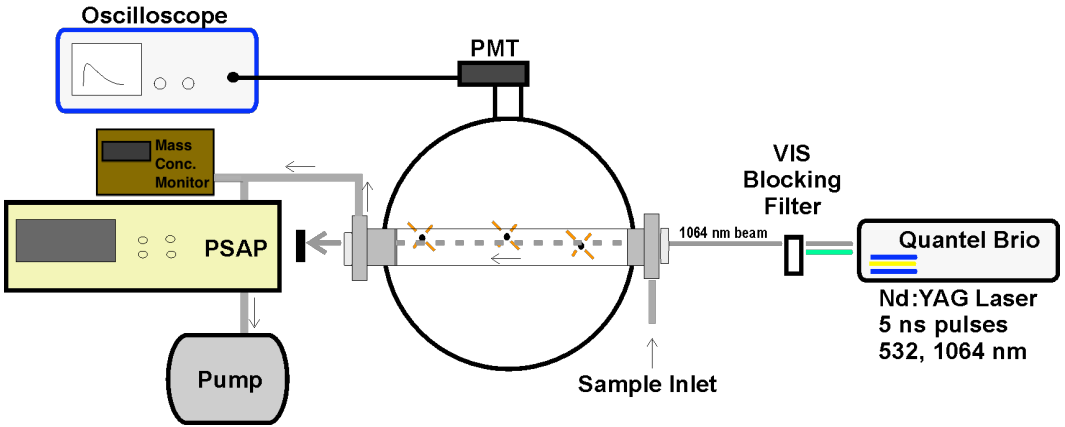

Fig. 1. Apparatus used for LII Measurements. The measurement chamber was an integrating sphere equipped with a transparent tube to contain the sample. A PSAP and mass concentration monitor was used to normalize LII signals observed to optical absorption at 530 nm or observed mass concentrations (mg m^{-3}).

AMTD
6, 5173–5194, 2013

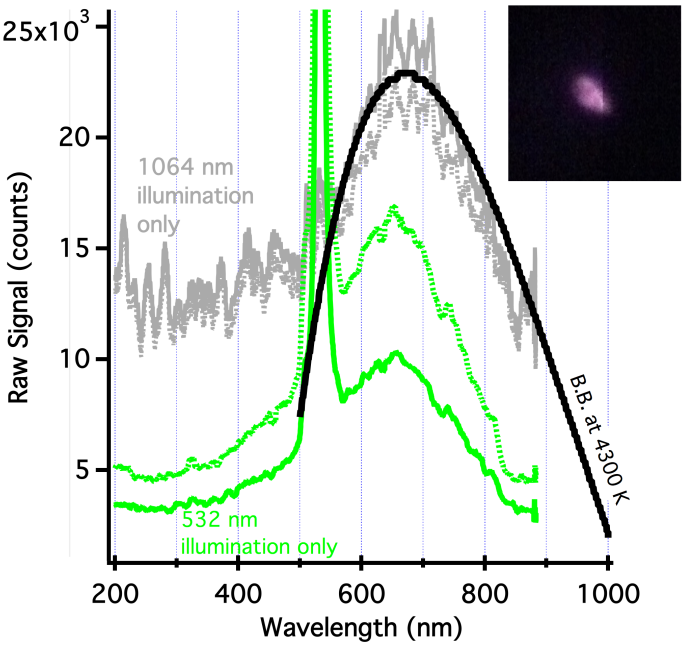

Fig. 2. Emission spectrum of Pullman (dashed lines) and Amarillo soil (solid lines) dusts during illumination with 532 or 1064 nm. Little difference in emission between soil types was noted. The large, sharp peak in the green traces is reflected laser light. The black trace plotted on a second y-axis (not shown) is representative of a blackbody at 4300 K. The photograph illustrates visible emission from dust when illuminated at 1064 nm. The image was recorded with a cell-phone camera.

AMTD
6, 5173–5194, 2013

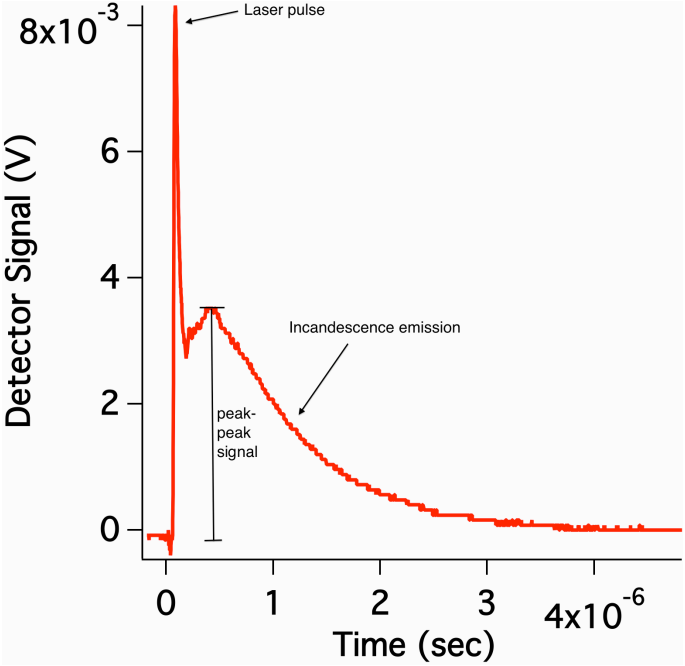

Fig. 3. Temporal response of Pullman dust LII signal. As observed, emission occurs for approx. 3 µs after the laser pulse. This is consistent with LII. The peak-peak signal indicated was used for quantitative measurements.

AMTD
6, 5173–5194, 2013

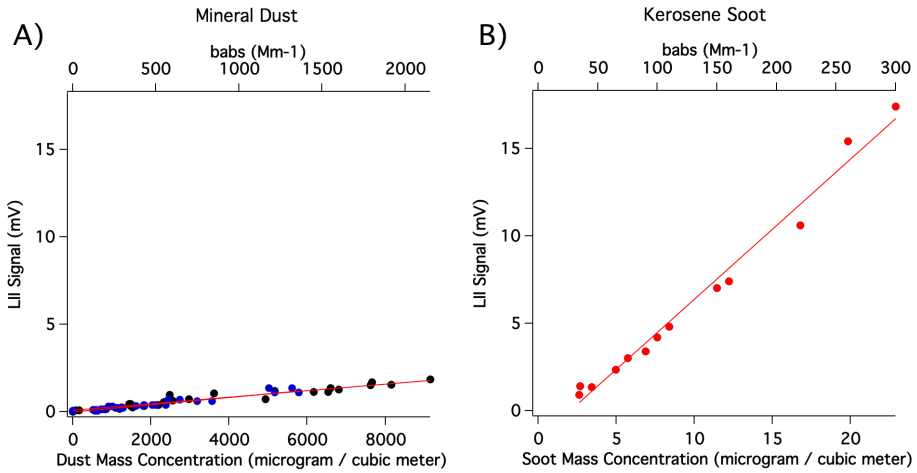

Fig. 4. Measured LII response of **(A)** Pullman and Amarillo mineral dust proxies and **(B)** kerosene soot as a function of estimated mass concentration and measured PSAP absorption coefficient. For this data, mass concentrations were determined through the absorption measurement and mass absorption cross-sections of 0.27, 0.25 and 13.1 $m^2\ g^{-1}$ for Amarillo dust, Pullman dust and soot, respectively. The observed slope for soot is 240–4600 times larger than the mineral dusts tested suggesting soot is far more effective at producing incandescence when compared to bulk mineral dust on a per-mass basis.

AMTD
6, 5173–5194, 2013

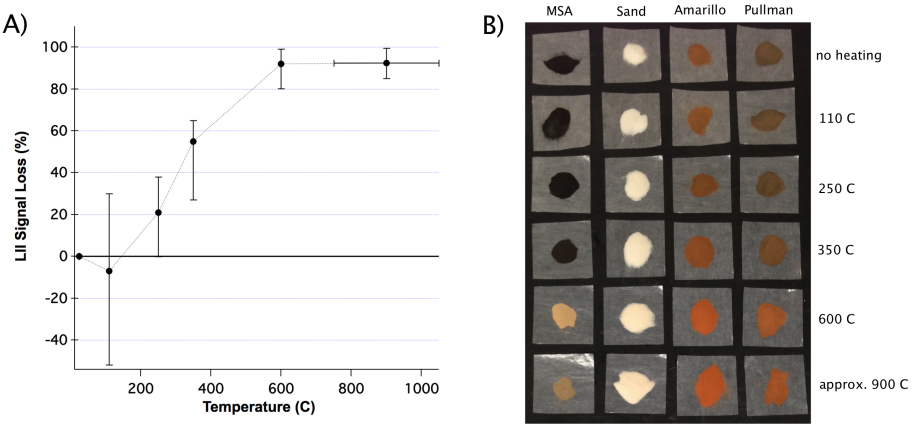

Fig. 5. (A) Plot of % LII signal loss vs. temperature at which the soil was heated. The measurement reference point was unheated soil of identical type. The data points represent the average loss observed for the four soil samples while the y-error bars represent the range of values observed. The x-error bar at 900 °C represents uncertainty in heating temperature since this sample was heated within a crucible in a Bunsen burner flame. **(B)** Photographs of soils after various heating steps. The most significant color changes occurred between 350–600 °C – the same temperature range in which BC oxidizes and is removed.

AMTD
6, 5173–5194, 2013

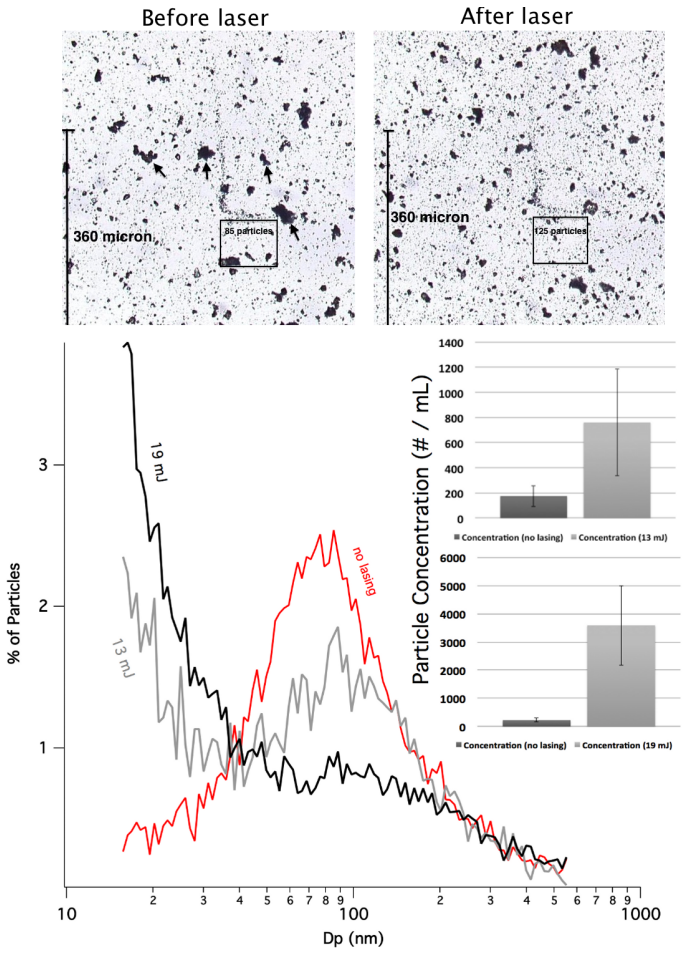

Fig. 6. Caption on next page.

AMTD
6, 5173–5194, 2013

Fig. 6. The photographs depict optical micrographs of Pullman soil dust deposited on a glass slide before and after laser irradiation with a combined 532 and 1064 nm beam at 22 mJ. A faint "L" shaped feature present near the center is evident in both images. Clear changes in the sample are noted after lasing. In addition, the boxed area contains roughly 50 % more particles for the lased sample. The bar graphs plot concentration of dispersed dust (# particles cm^{-3}) with and without laser illumination in the LII optical cell (both 532 + 1064 nm) at 13 and 19 mJ pulse energy. Large increases in particle concentration were observed during lasing. In addition, the SMPS size distribution illustrated a shift towards a large number of very small particles during lasing.

AMTD
6, 5173–5194, 2013